EVALUATING THE SEISMIC HAZARD IN NORTHERNMOST CHILE

I. Wong[(1)], M. Dober[(2)], S. Olig[(3)], and J. Bott[(4)]

[(1)] *Senior Principal Seismologist, Lettis Consultants International, wong@lettisci.com*
[(2)] *Senior Seismologist, AECOM, mark.dober@aecom.com*
[(3)] *President, Olig Seismic Geology, Inc., oligseismicgeo@gmail.com*
[(4)] *Engineering Geologist, California Geological Survey, Jacqueline.Bott@conservation.ca.gov*

Abstract

We have evaluated the probabilistic seismic hazard in northernmost Chile near its border with Bolivia. Chile is one of the most seismically active regions in the world as it is situated over the South American subduction zone. Northernmost Chile was the site of the 1877 **M** 9.0 Iquique earthquake and includes the northern Atacama fault. We evaluated the available geologic and seismologic data to develop a seismic source model that included 10 crustal faults, background crustal earthquakes, and the megathrust and intraslab zone of the South American subduction zone. Few active fault studies have been performed in northern Chile and so it is highly likely that there are Quaternary faults unaccounted for in our seismic source model. Therefore, the background crustal seismic source zone was characterized to include both possible blind faults as well as unmapped Quaternary faults that may have surface expression. The geometry of the megathrust was modeled as a dipping fault and recurrence intervals were based on the historical earthquake and tsunami record of the characteristic events. The record is relatively short and so the uncertainties are large. However, we judge the prevailing approach of calculating the recurrence based solely on the historical catalog and assuming a truncated exponential model as being inappropriate given that the megathrust more likely follows the characteristic or maximum magnitude recurrence models. We did assume a truncated exponential model for the intraslab source zone and the background crustal source zone given they are volumetric seismic sources containing numerous potential faults. We used state-of-the-art ground motion models for the crustal and subduction zone earthquakes including the NGA-West2 models. Assuming a soil site condition with a V_S30 of 350 m/sec, we performed a probabilistic seismic hazard analysis. For typical building code return periods of 475 and 2475 years, the peak horizontal ground accelerations ranged from 0.50 g to 0.92 g and 0.86 g to 1.71 g, respectively, for the cities of Tocopilla, Calama, and Antofagasta.

Keywords: seismic hazard; northernmost Chile; ground motion models; South American subduction zone

1. Introduction

Northernmost Chile is one of the most seismically active regions in the world (Figs. 1 and 2). The region was the site of one of the largest known earthquakes, the 1877 moment magnitude (**M**) ~9 Iquique event and it is expected that the earthquake will be repeated in the future. Late-Quaternary crustal faults capable of generating large earthquakes (**M** ≥ 6.5), such as the Atacama fault, are also located in the region (Fig. 3).

The primary objective of this study was to characterize the future levels of ground motions that will be exceeded at a specified probability in northernmost Chile at three selected cities by performing a probabilistic seismic hazard analysis (PSHA). Available geologic and seismologic data were used to evaluate and characterize potential seismic sources, the likelihood of earthquakes of various magnitudes occurring on those sources, and the likelihood of the earthquakes producing ground motions over a specified level. It should be noted that there are very significant uncertainties in the characterization of seismic sources and ground motions in northernmost Chile due to the

limited research in active faulting and ground motion modeling; these uncertainties have been incorporated into the PSHA. For input into the PSHA, seismic sources need to be defined and characterized and ground motion models (GMMs) selected. For the GMMs, we used models for crustal and subduction zone earthquakes.

The PSHA approach used in this study was based on the model developed principally by Cornell [1]. The calculations were made using the computer program HAZ45 developed by Norm Abrahamson. This program has been validated in the Pacific Earthquake Engineering Research (PEER) Center-sponsored projects [2, 3]. Epistemic uncertainties were addressed using logic trees.

2. Seismotectonic Setting and Historical Seismicity

Tectonically, the site is located on the South America plate, which overrides the actively subducting Nazca plate. At the latitudes of northernmost Chile, the Nazca plate is being subducted at a shallow dip (about 10° to 30°) (Fig. 4) and at a rate of 64 to 79 mm/yr. Northernmost Chile is located at the southern end of the "Big Bend" of the Peru-Chile subduction zone, between the latitudes of 15.5° to 22°S (Fig. 1). The sources of seismicity in Chile include shallow crustal faults (Fig. 3), both known and unknown, at depths of less than 30 to 40 km and the South America subduction zone megathrust and the Wadati-Benioff zone (Figs. 1 and 4). This section of the subduction zone has a history of large destructive earthquakes including the destructive 1868 **M** 9 Arica and 1877 **M** 9.0 Iquique earthquakes. Most of these earthquakes have generated destructive tsunamis [4].

A historical earthquake catalog was compiled for the region as shown in Fig. 2. The catalog covers the time period 1836 to 2019. Primary data sources included catalogs from the U.S. Geological Survey's National Earthquake Information Center (NEIC), Centro Regional de Sismologia para America del Sur (CERESIS), el Servicio Sismologico de la Universidad de Chile (GUC), the International Seismological Center (ISC), and the National Oceanic and Atmospheric Administration's (NOAA) National Geophysical Data Center database of significant earthquakes.

2.1 Significant Earthquakes

Since 1836, a total of 24 earthquakes larger than approximately **M** 7 have been recorded or reported to have occurred in the region (Fig. 2). Four very large earthquakes (**M** $\geq$ 7.7) have occurred along the subduction zone megathrust in 1877, 1995, 2007, and 2014 (Fig. 1). One very large intraslab earthquake (surface wave magnitude [M_S] 7.9) occurred in 2005 in Chiapa at a depth of 95 km within the subducting slab (Fig. 2).

2.1.1 1877 M 9 Iquique Earthquake

This **M** 9 earthquake which occurred on 9 May 1877 around Iquique is thought to have ruptured up to 510 km and has an estimated displacement of 10 m [4] (Fig. 1). The earthquake unleashed a destructive tsunami that spread throughout the Pacific Basin. This portion of the Peru-Chile subduction zone and that to the north (which ruptured in 1868 with an estimated **M** 9.0 event) last ruptured in 2014 (see below) but still may represent a seismic gap where another 1877 event may occur.

2.1.2 1995 M 8.0 Antofogasta Earthquake

The 30 July 1995 **M** 8.0 Antofogasta earthquake rupture extended south from Mejillones Peninsula to Paposo from a depth of 10 to 50 km along the subduction zone interface (Fig. 1). This event took place just south of the seismic gap where the 1877 earthquake occurred. The earthquake propagated from north to south as has been observed for other large earthquakes along this subduction zone [4].

2.1.3 2007 M 7.7 Tocopilla Earthquake

This large earthquake occurred on 14 November 2007 near the small town of Tocopilla, 150 km north-northeast of Antofogasta (Figs. 2 and 3). The earthquake hypocenter occurred at a depth of 38 km and is the result of reverse faulting and hence, can be categorized as a megathrust event. This earthquake occurred in the southern portion of the seismic gap which ruptured in 1877. The depth of the rupture zone, between about 35 and 50 km, explains the lack of a large tsunami being generated during this event.

2.1.4 2014 M 8.1 Pisagua Earthquake

The occurrence of the 2014 **M** 8.1 Pisagua earthquake was surprising in that it was located between the proposed 1868 and 1877 earthquake rupture areas [5] (Fig. 1). The event occurred in the curved section of the subduction zone that may have acted as a barrier for the 1868 and 1877 events and also as an isolated segment of the 2014 earthquake. The earthquake generated a tsunami that had a maximum height of 2 m.

2.2 Spatial Distribution of Earthquakes

Examination of the historical seismicity shows only a moderate level of crustal seismicity (Figs. 2 and 4). The intraslab seismicity is diffuse and distributed throughout the subducting Nazca plate. The plate appears to dip at a shallow angle of around 19 to 20 degrees and then steepens at a depth of about 100 to 150 km where the slab begins to dip at around 22 degrees (Fig. 4). A large percentage of intraslab earthquakes are occurring where the slab changes dip and is most likely related to the bending stresses within the subducting slab as it begins to dip more steeply (Fig. 4).

3. Seismic Source Characterization

The active and potentially active seismogenic crustal faults, the Peru-Chile subduction zone (both megathrust and instraslab zones), and background crustal seismicity are the seismic sources significant to northernmost Chile. Potentially significant active crustal faults were identified but it needs to be stressed that the inventory of active crustal faults in northern Chile is significantly incomplete. Few active fault investigations have been performed in northern Chile, and even fewer paleoseismic investigations have been conducted to decipher prehistoric earthquake rupture behavior. Much of our characterization is based on a compilation by Lavenu *et al.* [6]. We updated and supplemented this information with subsequently published fault studies in the region (e.g., [7, 8]). We emphasize that a systematic investigation to identify active and potentially active faults in northernmost Chile has not been performed.

3.1 Crustal Fault Sources

A total of 10 crustal fault sources were judged to be active and were characterized in the hazard model because they display evidence for Quaternary displacement [6] (Fig. 3). The faults generally strike north-south and are dominantly located along the coastal Cordillera, including the Atacama fault zone, which is a major strike-slip/oblique-slip fault that extends for over 500 km. (Fig. 3). In addition to faults in the coastal Cordillera, some relatively short and discontinuous Quaternary faults that generally show reverse slip have also been identified in parts of the Andean foothill region to the west [6] (Fig. 3).

Very little is known about the earthquake rupture behavior of Quaternary faults in northern Chile so our rupture models are relatively simple. For the longer Atacama fault zone, we considered a segmented rupture model based on the fault sections defined by Lavenu *et al.* [6]. However, given the large uncertainties in fault behavior, we also considered an unsegmented model where the entire

Atacama fault zone ruptures. Finally, we also considered an unsegmented model with floating ruptures on the northern and southern portions, based on apparent differences in faulting style [6].

Little is known about the seismogenic thickness of the crust in the region. Therefore, we assumed broad seismogenic depth distributions, which were primarily based on examination of the contemporary seismicity, with thinner crust in the forarc and thicker crust in the Andean arc. For all rupture models, all faults were modeled as planar sources that extend the full depth of the crust. Thus, fault dips for all of these rupture models are averages estimated over the full depth of the seismogenic crust. We assumed vertical to subvertical dips for the dominantly strike-slip Atacama fault zone, and moderate dips (45° to 70°) for the reverse and normal faults.

Maximum magnitudes for the faults were estimated using the relationships based on fault rupture length and rupture area of Wells and Coppersmith [9] for all types of faults. The preferred magnitude was weighted 0.6. To account for the various uncertainties in estimating maximum magnitudes, we also included ± 0.3 magnitudes (weighted 0.2 each) for all of our maximum magnitude distributions.

The timing of earthquakes on most faults in the region is unknown and so recurrence intervals for earthquake ruptures on faults are also unknown. Therefore, we used slip rates (in mm/yr) to characterize the rate of earthquake activity for crustal fault sources. Unfortunately, slip rates are also very poorly constrained. Regionally, the foreland fold and thrust belt of the Andes is shortening at a rate of about 10 mm/yr [10]. However, specific slip rates are unknown for the faults included in this analysis [6]. Therefore, slip rates for the thrust faults in the analysis were assigned based on comparison to better-studied faults in the region, specifically the Salar fault system, which is located in the Atacama basin about 15 to 35 km south of the Frontal Thrust fault of the Cordillera de la Sal [7]. Based on analysis of seismic profiles, drill holes, and geologic mapping, Jordan *et al*. [7] determined vertical slip rates throughout the Quaternary that have ranged from 0.1 to 2.0 mm/yr on the Salar fault, a high-angle, west-dipping reverse fault. On the basis of comparison with the geomorphic expression, length, continuity and structural relief to the Salar fault, we assumed broadly weighted slip-rate distributions for other thrust faults included in this analysis.

The Atacama fault zone has a long and complex deformation history stretching as far back as the Jurassic-early Cretaceous that may have included reactivating the zone with different styles of faulting (e.g., sinstral, dextral and vertical) (e.g., [11, 12]), and the current sense of slip remains controversial [6]. Quaternary slip rates are also very poorly constrained. Although 5-m-high Quaternary scarps are apparently documented, the net slip and ages are unknown [6]. Primarily based on comparison to the nearby Morro Mejilones fault, we assigned a preferred slip rate of 0.3 mm/yr to the Atacama fault zone and included a broad distribution spanning two orders of magnitudes to try to address the large uncertainties for this major fault zone. For the normal and strike-slip faults adjacent to the Atacama fault e.g., Cerro Fortuna, we assigned the same slip rate distribution as the Atacama fault. An outstanding issue is whether these are independent faults or if they rupture together with the Atacama fault? The characteristic, maximum magnitude, and truncated exponential recurrence models were used for all the crustal faults in the PSHA weighted 0.6, 0.3, and 0.1, respectively. All source parameters for the crustal faults are available from the authors.

3.2 Crustal Background Seismicity

Crustal background or random earthquakes are those events that can occur without an apparent association with a known or identified tectonic feature. Within the Andean crust of northernmost Chile, seismicity is distributed diffusely with no clear relationships with any geologic structures.

These faults are often called "blind" or "buried" faults. To address the likely incomplete identification of Quaternary faults in the region, the background crustal seismic source zone was characterized to include possible blind faults as well as unmapped Quaternary faults that may have surface expression. Whether this approach sufficiently accounts for the true hazard is uncertain given the short historical record. The hazard from such sources is incorporated into the PSHA through inclusion of areal source zones and Gaussian smoothing.

We estimated the maximum magnitude for the background earthquakes to be between **M** 7.0 and 7.5, weighted 0.7 and 0.3, respectively. Earthquakes larger than **M** 6.5 to 7.0 will typically be accompanied by surface rupture in regions where the seismogenic crustal thickness is on the order of 15 to 20 km and thus repeated events of this size will produce recognizable fault-related geomorphic features at the earth's surface. However, the higher magnitudes used in this PSHA reflect the fact that there are crustal faults in northernmost Chile that we have not accounted for. We include these unknown seismic sources as part of the background seismicity.

Earthquake recurrence is required to characterize the background earthquakes. Initially the crustal earthquakes were divided into seismotectonic provinces based on major morphologic elements of the Andean Cordillera. However, the number of independent earthquakes for some of the provinces was inadequate for calculating recurrence reliably and thus a single seismic source zone was used for all crustal events.

The recurrence relationship was estimated following the maximum likelihood procedure developed by Weichert [13] and estimated completeness intervals for the region (Fig. 5a). The relationship is in the form of the truncated exponential distribution for the occurrence of independent earthquakes. Dependent events were identified and removed from the historical catalog of crustal earthquakes. The resulting catalog for independent events was then used to develop the recurrence relationship. The recurrence curve is well constrained (Fig. 5a). However, because of the limited duration and incompleteness of the historical catalog, uncertainties in the recurrence parameters for the crustal background seismicity are large.

In addition to the traditional approach of using areal source zones with uniformly distributed seismicity, Gaussian smoothing [14] with a spatial window of 15 km was used to address the hazard from background seismicity and incorporate a degree of stationarity. We weighted the two approaches equally at 0.5 to compute the hazard from background seismicity in the PSHA.

3.3 Peru-Chile Subduction Zone

3.3.1 Megathrust

We developed a model of the Peru-Chile subduction zone that consists of three segments with the middle segment being the Arica-Antofagasta segment that ruptured in 1877 (Fig. 1). The model is based generally on the model of Nishenko [15] with modifications. Several investigators have recognized that the Peru-Chile subduction zone is segmented based on the historical record. Nishenko [15] defined the following segments nearest the site: (1) the Arica-Antofagasta (19°-24°S) segment that ruptured in 1877; (2) the Arica segment (19°-16.6°S) that ruptured in 1604 and 1868; and (3) the Antofagasta-Paposa segment, site of the 1995 earthquake. Okal *et al*. [16] believes the 1868 earthquake ruptured beyond the Nazca Ridge, which is a segment boundary in earlier models. In the Nishenko [15] model, this would be the boundary between the Arica and Camana segments. In this study, we extend the northern boundary of the 1868 segment to the north to 14.4°S latitude based on Okal *et al.* [16]. The boundaries for the 1877 segment are taken from the

estimated rupture area from Dewey *et al*. [17]. Finally, the 1995 segment is taken from the rupture area as estimated by Chlieh *et al*. [18] (Fig. 1).

We assume that the maximum earthquakes for the megathrust have occurred already in historical times and have thus adopted the estimated maximum magnitudes observed to date with their uncertainties. For the 1868, 1877, and 1995 segments, that would be **M** 9.0 ± 0.2, **M** 8.8 ± 0.2, and **M** 8.0 ± 0.2, respectively. If the section of the subduction zone that ruptured in 2014 is an independent segment, then it should be included explicitly in future hazard analyses. We addressed the hazard from the 2014 earthquake by modeling the smaller ruptures in the 1868 and 1877 segments using the exponential portion of the characteristic recurrence model (see following discussion).

The plate dips and maximum depths of the seismogenic megathrust along this portion of the subduction zone are generally uniform. Okal *et al*. [16] used a dip of 20° in their tsunami modeling of the 1868 earthquake. Delouis *et al*. [19] estimated a dip of 20° from focal mechanism analysis of the 2007 **M** 7.7 Tocopilla earthquake. However, based on observations of a portable microearthquake network, Comte *et al*. [20] estimate the plate dip to be shallow around 10° in the vicinity of Antofagasta to a depth of 30 km. Biggs *et al*. [21] favored a very shallow dip of 12° in their modeling of the 2007 Pisco earthquake and Giovanni *et al*. [22] used a dip of 14° in their modeling of the 2001 **M** 8.4 Arequipa earthquake. In contrast, Tavera *et al*. [23] estimated a dip of 28° based on aftershocks of the 2001 earthquake and 21° based on its focal mechanism. We adopt a dip of 17° ± 3° for the 1868 segment and 14° ± 4° for the 1877 and 1995 segments.

The maximum depth of the megathrust is not well constrained but it too is based on observations of seismicity. Tichelaar and Ruff [24] suggested that the maximum depth along the Peru-Chile megathrust was 36 to 41 km north of latitude 28°S. Comte and Suarez [25] suggested a maximum depth of 40 ± 10 km with no appreciable variations along strike. Delouis *et al*. [19] noted that aftershocks of the 2007 Tocopilla earthquake extended to a depth of 50 km. Tavera *et al*. [23] observed the 2001 aftershocks to extend to a depth of 60 km. Accurate aftershock locations of the 1995 Antofagasta earthquake place its downdip limit at 46 km [26] or 50 km [27]. We adopt a range of 50 ± 5 km for the PSHA.

We judge the common approach of calculating the recurrence for the megathrust based on the historical catalog of both intraslab and megathrust earthquakes and assuming a truncated exponential model as being inappropriate given that the megathrust more likely follows the characteristic or maximum magnitude recurrence models. We weighted the characteristic and maximum magnitude recurrence models 0.7 and 0.3, respectively. In terms of recurrence intervals of the 1868 segment, only two earthquakes (1604 and 1868) have ruptured the whole segment [16]. Thus the single recurrence interval is 264 years. In their evaluation of the tsunami risk of Pisco, Okal *et al*. [16] adopted a repeat time of 250 years for their “order-of-magnitude” calculations. We adopt a value of 260 years but with a large uncertainty of 100 years. As noted by Nishenko [15], there is no known predecessor of the 1877 event. Nishenko [15] compares this segment with a similar-sized southern Chile segment to the south that has an estimated recurrence interval of 111 years and the 1868 segment (264 years). Hence, we adopt a broad distribution of 200 ± 100 years for the 1877 segment. Finally, for the 1995 segment, we adopt a recurrence interval of 300 ± 100 years. This event, like the 1877 segment, has had no history of large earthquakes prior to 1995 and the historical record is probably complete for the largest events for at least the past 200 years.

3.3.2 Wadati-Benioff Zone

The largest known intraslab earthquake in the region was the 2005 **M** 7.7 Chiapa earthquake. Based on the 1970 **M** 7.9 Chimbote, Peru event, the intraslab earthquake within the subducting plate has been assumed to have a maximum magnitude of **M** 8.0 ± 0.2 beneath the northernmost Chile. The plate thickness is assumed to be 45 ± 10 km based on Norabuena *et al*. [28]. We adopt a single intraslab region for the Peru-Chile subduction zone.

Similar to the approach taken for the crustal background seismicity, the recurrence was estimated for the intraslab zone assuming the truncated exponential model. The intraslab recurrence curve is well constrained and predicts recurrence intervals for **M** 6.0 and greater and **M** 7.0 and greater of about 1 and 15 years, respectively (Fig. 5b). The *b*-value was varied by ± 0.1 in the PSHA as was done for the crustal background zone.

4. Ground Motion Models

In this evaluation, the PEER Next General Attenuation (NGA)-West2 models for the crustal earthquakes in tectonically active regions by Abrahamson *et al*. [29], Chiou and Youngs [30], Campbell and Bozorgnia [31], and Boore *et al*. [32] were used in the PSHA. These GMMs have been shown to be applicable to other regions worldwide.

Arango *et al*. [33] evaluated a set of global and regional subduction GMMs for their applicability to Peru-Chile and Central America. Their evaluation utilized a database of strong motion data from Peru and Chile. We used two well-known GMMs for subduction zones that post-date the Arango *et al*. [33] study: Abrahamson *et al*. [34] and Montalvo *et al*. [35]. The former is a global model and latter is based on strong motion data from Chile. We weighted the GMMs 0.6 and 0.4, respectively.

5. Hazard Results

To characterize the probabilistic hazard in northernmost Chile, we calculated it for three major cities: Tocapillo and Antofagasta on the coast and inland Calama (Figs. 2 and 3). The hazard was calculated for a firm soil site condition with V_S30 (time-averaged shear-wave velocity in the top 30 m) of 350 m/sec. Fig. 6 shows the deaggregated hazard for horizontal peak ground acceleration (PGA) and 1.0 sec spectral acceleration (SA) by seismic sources for Antofagasta. The controlling seismic source at PGA is the intraslab zone. The next most important seismic source is the Antofagasta-Paposa segment of the megathrust, source of the 1995 earthquake on which Antofagasta is located above. The hazard contributions for different sources are similar for all three cities even though Calama is further inland. Also, although the two coastal cities are astride or adjacent to the Atacama fault, it is not a significant contributor to hazard due to its apparently relatively low slip rate (~0.3 mm/yr) (Fig. 6).

As anticipated, the hazard in northernmost Chile is quite high compared to other regions worldwide. On Fig. 7, the hazard is shown for PGA and 1.0 sec SA for all three cities. The figure shows that the hazard for Tocapilla is the highest, followed by coastal Antofagasta, and then inland Calama. The PGA and 1.0 sec SA hazard are shown in Table 1 for the return periods of 475, 975, and 2,475 years.

Table 1 – Mean Probabilistic Hazard

Return Period	475 years		975 years		2,475 years	
City	PGA (g)	1.0 sec SA (g)	PGA (g)	1.0 sec SA (g)	PGA (g)	1.0 sec SA (g)
Antofagasta	0.79	0.55	1.07	0.77	1.55	1.10
Calama	0.50	0.33	0.64	0.44	0.86	0.62
Tocopilla	0.92	0.79	1.23	1.10	1.71	1.57

6. References

[1] Cornell, CA (1968): Engineering seismic risk analysis. *Bulletin of the Seismological Society of America*, **58**, 1583-1606.

[2] Thomas, PA, Wong, IG, Abrahamson, NA (2010): Verification of probabilistic seismic hazard analysis software programs. *Pacific Earthquake Engineering Research Center, Report 2010/106*, 161.

[3] Hale, C, Abrahamson, N, Bozorgnia, Y (2018): Probabilistic seismic hazard analysis code verification. *PEER Report 2018/03*, Pacific Earthquake Engineering Research Center, Berkeley, USA.

[4] Barrientos, SE (2007): Earthquakes in Chile, in Moreno, T and Gibbons, W (eds.) The Geology of Chile. *The Geological Society of London*, 263-287.

[5] Shrivastava, MN, Gonzalez, G, Moreno, M, Soto, H, Schurr, B, Salazar, P, Baez, JC (2019): Earthquake segmentation in northern Chile correlates with curved plate geometry. *Scientific Reports*, 1-10.

[6] Lavenu, A, Thiele, R, Machette, MN, Dart, RL, Bradley, L, Haller, KM (2000): Maps and database of Quaternary faults in Bolivia and Chile. *U.S. Geological Survey Open-File Report 00-283*, 46.

[7] Jordan, TE, Munoz, N, Hein, M, Lowenstein, T, Godfrey, L, Yu, J (2002): Active faulting and folding without topographic expression in an evaporate basin, Chile. *Geological Society of America Bulletin*, **114**, 1406-1421.

[8] Marquardt, C, Braucher, R, Ritz, J-F, Philip, H, Bourles, D, Lavenu, A, Delouis, B, Ortlieb, L (2002): Upper Quaternary slip rates along Mejillones fault, Northern Chile (23°S), estimated using ^{10}BE exposures ages. *Simposio Internacional de Geologia Ambiental para Planificacion del Uso del Territorio, Puerto Varas*, 89-92.

[9] Wells, DL, Coppersmith, KJ (1994): New empirical relationships among magnitude, rupture length, rupture width, rupture area, and surface displacement. *Bulletin of the Seismological Society of America*, **84**, 974-1002.

[10] Dewey, J, Lamb, S (1992): Active tectonics of the Andes. *Tectonophysics*, **205**, 79-95.

[11] Arabasz, WJ (1971): Geologic structure of the Taltal area, northern Chile, in relation to the earthquake of December 28, 1966. *Bulletin of the Seismological Society of America*, **58**, 835-842.

[12] Brown, M, Diaz, F, Grocott, J (1993): Displacement history of the Atacama fault system 25°00'S-27°00'S, northern Chile. *Geological Society of American Bulletin*, **105**, 1165-1174.

[13] Weichert, DH (1980): Estimation of the earthquake recurrence parameters for unequal observation periods for different magnitudes. *Bulletin of the Seismological Society of America*, **70**, 1337-1346.

[14] Frankel, A (1995): Mapping seismic hazard in the central and eastern United States. *Seismological Research Letters*, **66**, 8-21.

[15] Nishenko, SP (1991): Circum-Pacific seismic potential 1989-1999. *Pure and Applied Geophysics*, **135**, 169-259.

[16] Okal, EA, Borrero, JC, Synolakis, CE (2006): Evaluation of tsunami risk from regional earthquakes at Pisco, Peru. *Bulletin of the Seismological Society of America*, **96**, 1634-1648.

[17] Dewey, JW, Silva, WJ, Tavera, H (2003): Seismicity and tectonics, Chapter 1 in Southern Peru Earthquake of 23 June 2001 Reconnaissance Report. *Earthquake Spectra Supplement*, A to **19**, 1-10.

[18] Chlieh, M, de Chabalier, JB, Ruegg, JC, Armijo, R, Dmowska, R, Campos, J, Feigl, KL (2004): Crustal deformation and fault slip during the seismic cycle in the North Chile subduction zone, from GPS and InSAR observations. *Geophysical Journal International*, **158**, 695-711.

[19] Delouis, B, Pardo, M, Legrand, D, Monfret, T (2009): The Mw 7.7 Tocopilla earthquake of 14 November 2007 at the southern edge of the northern Chile seismic gap: rupture in the deep part of the coupled plate interface. *Bulletin of the Seismological Society of America*, **99**, 87-94.

[20] Comte, D, Pardo, M, Dorbath, L, Dorbath, C, Haessler, H, Rivera, L, Cisternas, A, Ponce, L (1992): Crustal seismicity and subduction morphology around Antofagasta, Chile: preliminary results from a microearthquake survey. *Tectonophysics*, **205**, 13-22.

[21] Biggs, J, Robinson, DP, Dixon, TH (2009): The 2007 Pisco, Peru, earthquake (M 8.0): Seismology and geodesy. *Geophysical Journal International*, **175**, 657-669.

[22] Giovanni, MK, Beck, SL, Wagner, L (2002): The June 23, 2001 Peru earthquake and the southern Peru subduction zone. *Geophysical Research Letters*, **29**, 14-1-14-4.

[23] Tavera, H, Fernandez, E, Bernal, I, Antayhua, Y, Aguero, C, Rodriguez, H, Vilcapoma, L, Zamudio, Y, Portugal, D, Inza, A, Carpio, J, Ccallo, F, Valdivia, I (2006) The southern region of Peru earthquake of June 23, 2001. *Journal of Seismology*.

[24] Tichelaar, BW, Ruff, LW (1991): Comment on seismic coupling along the Chilean subduction zone. *Journal of Geophysical Research*, **98**, 15,825-15,828.

[25] Comte, D, Suarez, G (1995): Stress distribution and geometry of the subducting Nazca plate in northern Chile using teleseismically recorded earthquakes. *Geophysical Journal International*, **122**, 419-440.

[26] Husen, S, Kissling, E, Fluch, E, Asch, G (1999): Accurate hypocenter determination in the seismogenic zone of the subducting Nazca Plate in northern Chile using a combined on-/offshore network. *Geophysical Journal International*, **138**, 687-701.

[27] Delouis, B, Monfret, T, Dorbath, L, Pardo, M, Rivera, L, Comte, D, Haessler, H, Caminade, JP, Ponce, L, Kausel, E, Cisternas, A (1997): The Mw=8.0 Antofagasta (Northern Chile) earthquake of 30 July 1995: a precursor to the end of the large 1877 gap. *Bulletin of the Seismological Society of America*, **87**, 427-445.

[28] Norabuena, EO, Snoke, JA, James, DE (1994): Structure of the subducting Nazca plate beneath Peru. *Journal of Geophysical Research*, **99**, 9215-9226.

[29] Abrahamson, NA, Silva, WJ, Kamai, R (2014): Summary of the ASK14 ground-motion relation for active crustal regions. *Earthquake Spectra*, **30**, 1025-1055.

[30] Chiou, B-SJ, Youngs, RR (2014): Update of the Chiou and Youngs NGA ground motion model for average horizontal component of peak ground motion and response spectra. *Earthquake Spectra*, **30**, 1117-1153.

[31] Campbell, KW, Bozorgnia, Y (2014): NGA-West2 ground motion model for the average horizontal components of PGA, PGV, and 5%-damped linear acceleration response spectra. *Earthquake Spectra*, **30**, 1087-1115.

[32] Boore, DM, Stewart, JP, Seyhan, E, Atkinson, GM (2014): NGA-West2 equations for predicting PGA, PGV, and 5%-damped PSA for shallow crustal earthquakes. *Earthquake Spectra*, **30**, 1057-1085.

[33] Arango, MC, Strasser, FO, Bommer, JJ, Cepeda, JM, Boroschek, R, Hernandez, DA, Tavera, H (2012): An evaluation of the applicability of current ground-motion models to the South and Central American subduction zones. *Bulletin of the Seismological Society of America*, **102**, 143-168.

[34] Abrahamson, N, Gregor, N, Addo, K (2016): BC Hydro ground motion prediction equations for subduction earthquakes. *Earthquake Spectra*, **32**, 23-44.

[35] Montalvo, GA, Bastías, N, Rodriguez-Marek, A (2017): Ground-motion prediction equation for the Chilean subduction zone. *Bulletin of the Seismological Society of America*, **107**, 901-911.

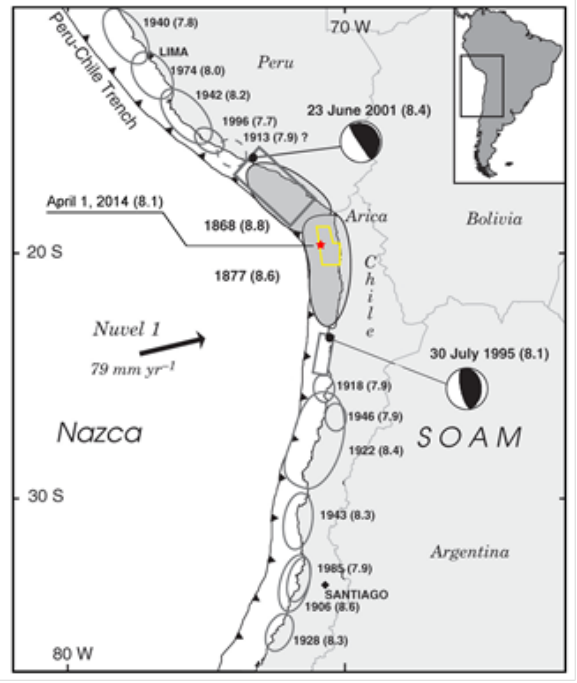

Fig. 1 – Large zone earthquakes along Peru-Chile subduction zone (**M** ≥ 7.0), 1868-2019. Modified from Chlieh *et al*. (2004).

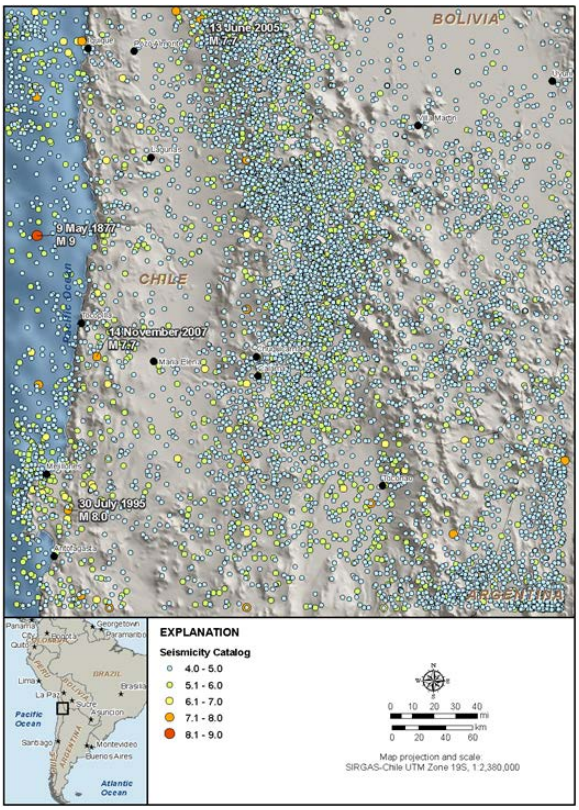

Fig. 2 – Historical seismicity of northernmost Chile, 1836-2019.

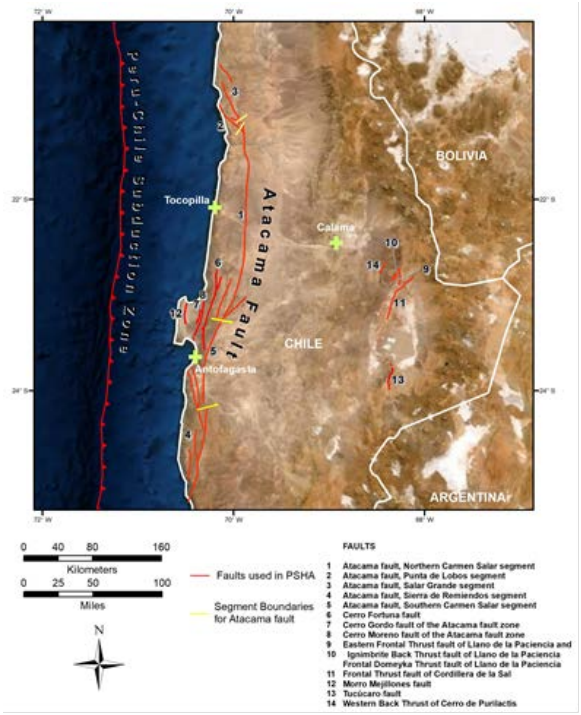

Fig. 3 – Crustal faults included in hazard analysis.

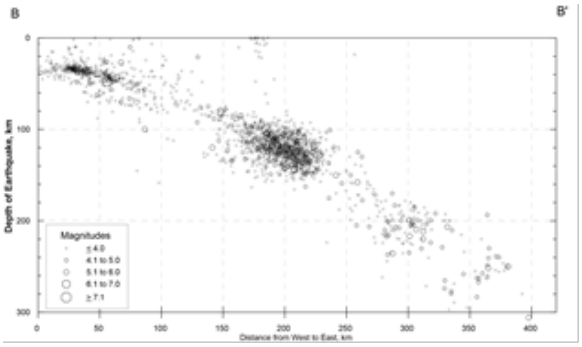

Fig. 4 – Cross-section of well-located earthquakes across the South American subduction zone.

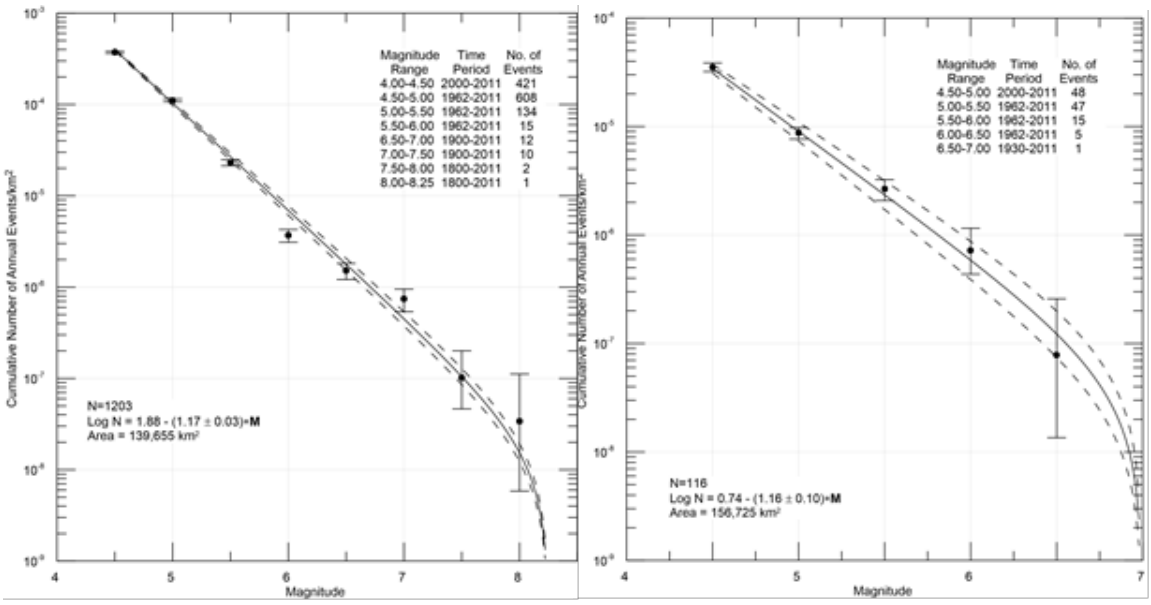

Fig. 5 – Recurrence for the (a) crustal and (b) intraslab earthquakes.

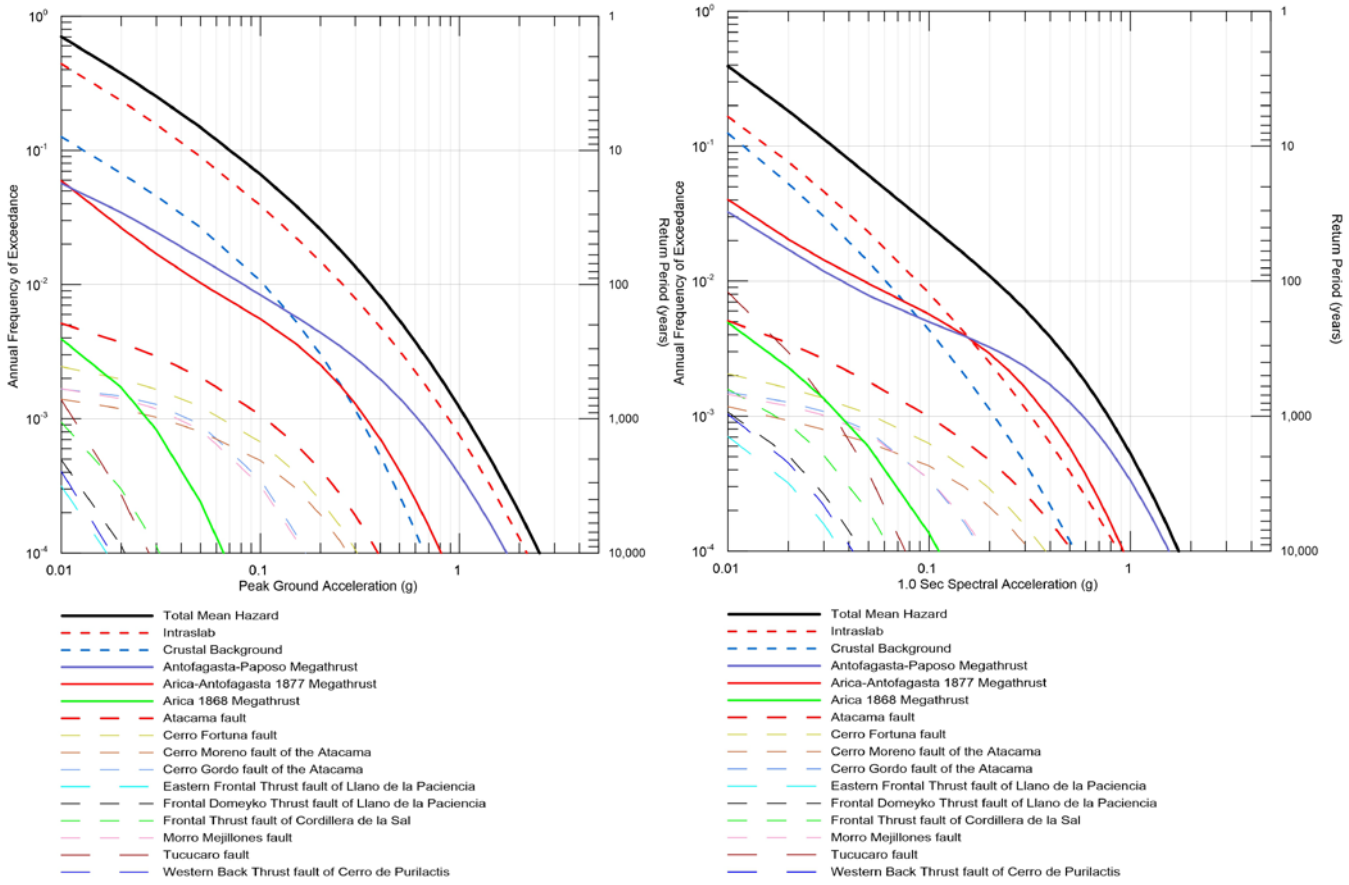

Fig. 6 – Deaggregated (a) PGA and (b) 1.0 sec SA hazard curves by seismic source for Antofagasta.

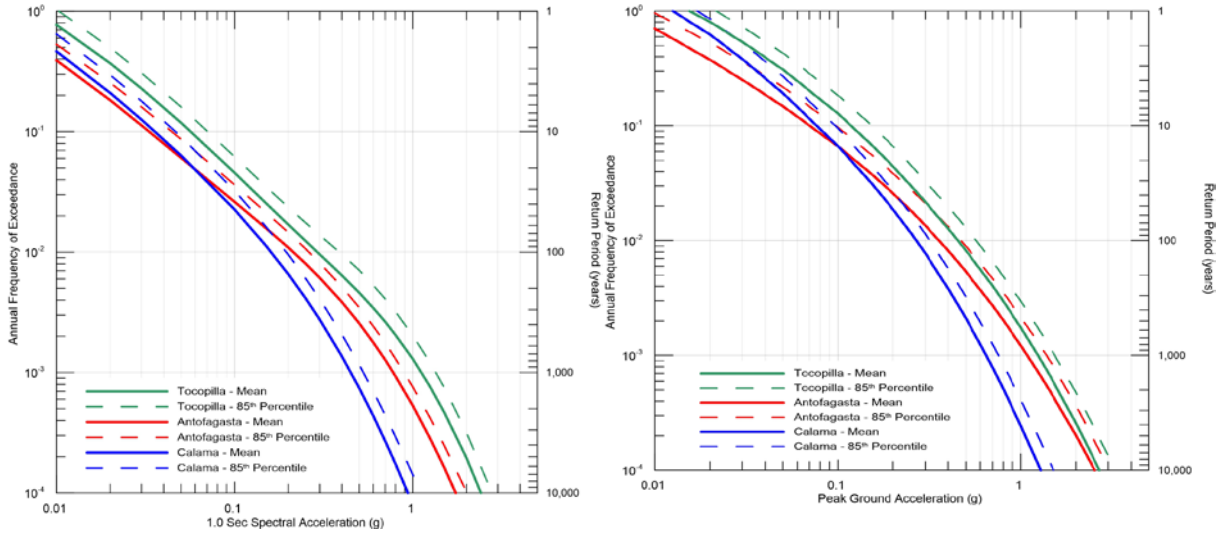

Fig. 7 – Hazard curves for (a) PGA and (b) 1.0 sec SA for the three cities.

